Frequency modulated optical feedback interferometry for nanometric scale vibrometry

Ajit Jha[1,2], Francisco J. Azcona[1], *Student Member, IEEE*, Santiago Royo[1], *Member, IEEE*,

Abstract—We demonstrate a novel method which makes efficient use of laser nonlinear dynamics when subject to optical self injection for sub-wavelength displacement sensing purposes. The proposed methodology combines two different phenomena taking place inside the laser cavity: optical self injection, which results in optical feedback interference, and laser continuous wave frequency modulation, giving rise to a wavelength sweeping effect in the laser's emission. We present a combination of these phenomena to measure vibration amplitudes below $\lambda/2$ with resolutions of a few nanometers, bandwidth dependent upon the distance of external target, amplitude and frequency of current modulation. The basic theoretical details and a mathematical model are presented for the developed measurement principle. Experimental results, with the system working as a vibrometer to measure a target vibration of amplitude $\lambda/5$ **(137.5 nm)** with mean peak to peak error of 2.4 nm just by pointing the laser diode onto the target and applying some signal processing is also demonstrated.

Index Terms—Optical feedback, Doppler frequency, optical sensors, nano displacement sensing, injection locking.

I. INTRODUCTION

AS described by Lang and Kobayashi [1], when the coherent light reflected from an external target is self-injected into the laser's cavity, then beating of time delayed optical field from distant target and field inside its cavity cause the laser to enter into multi stable states. Depending upon the feedback field self-injected into the cavity, several applications have been developed in the last decade. When the feedback strength is high, the laser diode (LD) reaches a chaotic region, which has been used for encrypted optical communications [2]. On the other hand, under moderate or weak feedback conditions, the LD output power experiences periodic fluctuations with a period equivalent to half emission wavelength ($\lambda/2$), which can be associated to interference fringes, thus leading to the concept of optical feedback interferometry (OFI).

Classic OFI methods are limited to the measurement of displacements larger than $\lambda/2$. In its origins, the fringe counting method enabled a $\lambda/2$ resolution, as described by Donati in [3]. During the last two decades, the increase of accuracy and resolution has been a driver of the research in the field [4]–[6]. The capability to measure vibration displacements smaller than $\lambda/2$ was recently demonstrated for the first time [7] using mechanical modulation and a double laser setup.
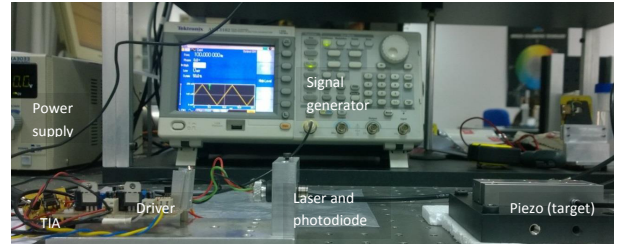
Fig. 1: Experimental set-up for proposed methodology. (TIA: Trans-Impedance Amplifier).

In that approach, the bandwidth of the sensor was dependent upon the product of the frequency and amplitude of the linear mechanical stage used to produce a reference OFI signal. The use of a mechanical modulator with a linear response increased the sensor's cost and size while limiting the measurement bandwidth.

To overcome these problems, we propose a novel approach that takes advantage of the finite non-zero linewidth enhancement factor (α) that couples the laser's amplitude and frequency modulations, in order to replace the mechanical modulation depicted in [7] by an electronic modulation. The developed method introduces two main advantages over [7]. First, the setup is simplified since the use of a second laser and of external mechanical elements to provide the modulation is no longer necessary. This reduces the cost and size of the sensor while making it comparable to classic OFI applications. The use of only one laser also reduces the possibility of bias in the measurement introduced by the difference of the physical properties between each LD or its circuitry. Second, the bandwidth and resolution of the proposed method are dependent only upon the LD electronic and optical parameters, in contrast to the mechanical scheme described before. This, in turn, allows to reach larger bandwidths since the method is no longer limited by mechanical constraints.

In the following sections we describe the working principle of a proposed optical sensor based on OFI effects induced by continuous wave frequency modulation (CWFM-OFI), including the methodology to calculate the target vibration waveform - amplitude and the frequency bandwidth of sensor.

II. SYSTEM DESCRIPTION AND THEORY

The proposed concept of the experiment is shown in Fig.1. First, a periodic current modulation is applied while the target is kept stationary. When the current feeding the laser is modulated, not only the intensity of the emitted signal is changed, but also its emission wavelength, because of the coupling between amplitude and frequency modulation, denoted by α parameter. To attain linear induced wavelength changes, a

triangular wave is used as modulation signal. Under these conditions, the laser can be thought as a multi-wavelength source whose wavelength changes with time proportionally to the injected current. The light emitted by the laser then hits the stationary target and part of the emitted light is back reflected into the cavity, where it interferes with the standing wave already present in the cavity, producing consecutive interference fringes in the emitted power with a phase difference of 2π between them.

The optical feedback signal obtained consists of a series of small ripples, caused by the beating of the time delayed reflected electric field with the emitted field inside the cavity, superimposed onto the ramp of the power signal modulated by the intensity as shown in Fig. 2(a). The signal is then subjected to a differentiation which separates the ripples caused by interference from the ramp caused by modulation. It has been shown that the number of fringes which appear on the ramp depend upon the round trip time delay (distance between the laser diode and the target) and upon the wavelength peak to peak change caused by the modulation current [6]. We call this the *reference case* and the fringes produced *reference fringes*. In experimental signals, after applying differentiation, the time of occurrence of each fringe will be noted and recorded.

We know that each $\lambda/2$ target displacement produces an interference fringe in the signal [1], [3]. Thus, if the target vibration amplitude is smaller than $\lambda/2$, no additional fringes are created as a result of the target motion. Even though the total number of fringes remains constant, the target motion changes the frequency seen by the laser due to the change in optical path difference, in the equivalent to a Doppler shift in the frequency domain. Thus, when compared to the former case, the new set of fringes will be shifted in time proportionally to the optical path change. From this point onward, we refer to this case as *vibration case*, and to its fringes as *vibration fringes*. It will be shown that it is possible to extract the complete information of the target displacement by comparing the reference and vibration cases. Mathematically, all parameters related to the *reference case* will be denoted by subscript *r* and the *vibration case* by subscript *v*. The excess phase ϕ_x and the emitted power P_x (with $x = [r, v]$) equations that govern both cases are defined by [8]

$$\phi_r(t) = 2\pi\tau_{ext}(f_{cr} - (f_{th} + i_m(t)\Omega_f))$$
$$+ C\sin(2\pi f_{cr}\tau_{ext} + \tan^{-1}\alpha) = 0, \tag{1}$$

$$P_r(t) = P_{ro}\cos(2\pi f_{cr}(t)\tau_{ext}), \tag{2}$$

$$\phi_v(t) = 2\pi\tau_{ext}(t)(f_{cv} - (f_{th} + i_m(t)\Omega_f))$$
$$+ C\sin(2\pi f_{cv}\tau_{ext}(t) + \tan^{-1}\alpha) = 0, \tag{3}$$

$$P_v(t) = P_{vo}\cos(2\pi f_{cv}(t)\tau_{ext}(t)), \tag{4}$$

where L_{ext} is the stationary distance from the laser to the target, and $L_{ext}(t) = L_{ext} + a(t)$, with $a(t) = A_t\cos(2\pi f_t t)$ describes a target motion with peak amplitude and frequency A_t and f_t, respectively. $\tau_{ext} = 2L_{ext}/c$ is the external round trip time for the reference case, $\tau_{ext}(t) = 2L_{ext}(t)/c$ the round trip time for the vibration case, f_{cr} and f_{cv} are the emission frequency of the laser after feedback for the reference and vibration case respectively, f_{th} is the standalone laser frequency at its operating point when no feedback is present,

TABLE I: Simulation parameters

| Parameters	Value
Distance of external target from laser (L_{ext}) (forward path)	0.3 m
Peak to peak modulating current ($I_m(pp)$)	1.5 mA
Modulation frequency (f_m)	100 Hz
Target vibration amplitude (pp) (A_m)	$\frac{\lambda}{10}$
Target vibration frequency (f_t)	200 Hz
Frequency modulation coefficient (Ω_f) [8]	-3 GHz/mA
Feedback strength (C)	0.9
Emission wavelength of laser (λ_{th})	692 nm
line width enhancement factor (α)	3
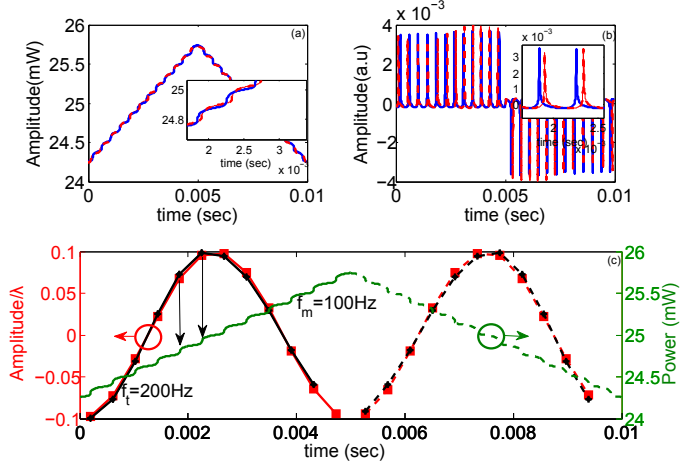
Fig. 2: Simulation results. (a) Emitted power variations in reference (blue solid) and vibration (red dash) cases (inset gives the magnified view). (b) Shift in fringes in both cases. (c) Target waveform reconstructed (black star) compared with the reference (red square). Arrows explains the formation of sampling points from fringes. By symmetry of modulation signal, processing any one ramp gives information about target vibration, making other ramp redundant.

$i_m(t)$ is the triangular AC modulation current driving the laser, Ω_f is the frequency coefficient of laser, C is the feedback strength, P is the emission power of the laser under feedback, with a total amplitude of P_{ro} and P_{vo} for the reference and vibration cases.

Simulations of performance based on Eq. (1) - (4) were carried out using the laser diode parameters listed in Table I. The goal of the simulation was to prove the appearance of power shifts in time between the reference and vibration cases. Nonlinear equations Eq. (1) and Eq. (3) were solved numerically to find f_{cr} and f_{cv} respectively. Then the corresponding power fluctuations were calculated using Eq. (2) and Eq. (4). Simulation results are presented in Fig. 2(a) and 2(b), which show a significant shift of the emission power related to the target motion.

A. Displacement Calculations

Now we will calculate the target displacement out of the the time shift between vibration and reference fringes. It is to be noted that the phase difference between each consecutive fringe is equivalent to a 2π phase change, which in OFI can be related to $\lambda/2$ if a displacement is present. Thus, the fraction of time shift on the vibration fringes relative to the reference fringes multiplied by $\lambda/2$ is equivalent to the target displacement. Let $\mathbf{t_r^n}$, $\mathbf{t_v^n}$, $\mathbf{t_{rv}^n}$, $\mathbf{t_{rr}^{n-1}}$ be vectors containing the recorded values of the time of occurrence of the reference and vibration fringes, the time difference between corresponding

fringes, and the time difference between consecutive reference fringes obtained in half modulation period. where the superscript is the number of elements in the considered vector, t_{xk} is the moment of occurrence of the kth fringe. Thus, the target displacement $\mathbf{A_{t,rec}}$ can be computed simply using

$$\mathbf{A_{t,rec}} = \frac{\mathbf{t_{rv}^{n-1}}}{\mathbf{t_{rr}^{n-1}}} \times \lambda/2 \qquad (5)$$

Using Eq. (5), the target waveform is reconstructed , shown in Fig. 2(c). It is worth noting, that, since the target vibration is twice the modulation frequency, the entire target waveform lie in one ramp (half period) of the modulation signal with arrow illustrating that each fringe corresponds to a measurement point. So it is desirable to process one of the ramp for target vibration related information.

B. Frequency Bandwidth

Let $f_m = \frac{1}{T_m}$ be the modulation frequency of current to the laser. In time $T_m/2$ (considering only one ramp of modulation signal; further explained in section III), we have N fringes giving $N-1$ sample points. Thus the sampling rate for target reconstruction is given by $f_{s,rec} = (2Nf_m - 1)$. From Nyquist theorem, the maximum frequency that can be reconstructed is half the sampling rate and using $2Nf_m >> 1$, can be approximated as $f_{t,rec} \simeq Nf_m$. We see that the maximum frequency of target vibration that can be reconstructed using the proposed sensor is dependent upon the product of modulation frequency and the number of fringes. Hence keeping the number of fringes N constant, the frequency of target vibration that can be detected is directly proportional to the modulation frequency i.e.$f_{t,rec} \propto f_m$. Since, a laser can be modulated at larger frequencies (MHz) keeping significant frequency deviation [9] as compared to mechanical vibration of laser in [7], this method gives wider bandwidth as compared to [7]. This also demonstrates the fact that the sensor's bandwidth that was limited by the bandwidth of piezo in former is now solely determined by the properties (maximum modulation frequency) of laser used and hence extending the bandwidth of sensor as compared to former.

III. EXPERIMENT AND RESULTS

Experimentally, a Hitachi HL6501 0.65 μm band AlGaAsP laser diode (LD) with a multi-quantum well (MQW) structure was used to test the method. The emission wavelength was measured with Instrument System's SPECTRO 320(D) R5 unit. The laser was then directly modulated to obtain the desired frequency chirp. Since under this operating conditions the LD may show mode hopping, a detailed analysis of its spectral characteristics as a function of the injection current was performed to locate the optimal operating point as shown in Fig. 3, whose measurements were performed repetitively in stable working conditions. The LD operating point was selected as I_{th} = 48 mA with λ_{th} = 692.5 nm. The laser is kept powered on and under stable working conditions when acquiring the reference and vibration measurements. To produce the frequency chirp, the LD is fed using a triangular current modulation with value at the operating point (I_{th}) peak to peak amplitude of 250 mV (0.2 mA) and a frequency of f_m = 100 Hz. The LD is focused on the target using a
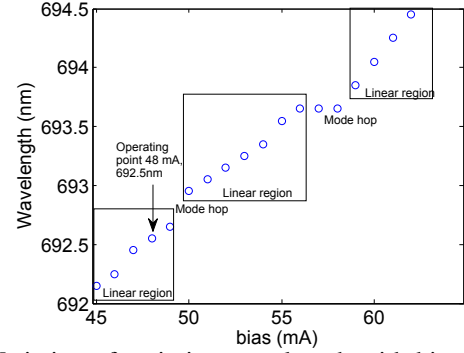

Fig. 3: Variation of emission wavelength with bias current.

Thorlabs lens 352240 with focal length of 8 mm and numerical aperture of 0.5 placed at a distance of 3.5 mm from the laser. A piezoelectric linear stage PI-LISA (P-753.3CD) placed at a distance (forward path) of 12 cm from the laser is used as target; the stage includes an embedded capacitive sensor with a resolution of 0.2 nm [10] which is used for comparing the obtained results. Previous to each measurement, the laser is set to work in the weak feedback region and it is allowed to attain a stable state. To dissipate the heat produced by the LD, the laser is mounted on an aluminium platform.

In a first step, a measurement of the reference case is acquired and denoised using a sym6 wavelet transform [11] and, then, the time of occurrence of the fringes is noted. Next, the target is set into vibration by applying to the AC sinusoidal signal with amplitude 55 mV and frequency 200 Hz (so that entire target vibration waveform lie in one ramp of modulation signal) to the piezoelectric stage using a signal generator, resulting in a 137.5 nm displacement measured by the embedded capacitive sensor [10]. The choice of target vibration frequency of 200 Hz was chosen as a proof of concept accompanied by simulations and theoretical proof and limited by the piezo. Due to the target motion, the optical path difference between laser and target changes resulting in a shift of the fringes when compared to the reference case. As in the reference case, the signal is acquired, denoised and the time of occurrence of the fringes is recorded. An example of typical experimental results is shown in Fig. 4. The fringe shift is easily appreciated and will be used to recover the target amplitude and frequency of vibration.

Once the time of occurrence of each fringe is computed for the reference and vibration cases, the target displacement is calculated using Eq. (5). Fig. 5 shows the experimental target displacement retrieved corresponding to the detected fringes resulting from a single oscillation of the target presented in Fig. 4, compared with the data obtained from the embedded capacitive sensor. It should be noted that only one ramp is processed to get the full period of target waveform (as the target vibration frequency is twice that of modulation frequency). The experiment was performed nine times under equivalent conditions. The mean error (pp) was 2.4 nm. For conciseness, only five measurements are listed in Table II. However, the t-test was carried on N_s = 9 samples with the degree of freedom $df = 2N_s - 2 = 16$ and significance level α_s = 0.05. Under these conditions, the probability of obtaining sample data if null hypothesis were true is $p = 0.92$.
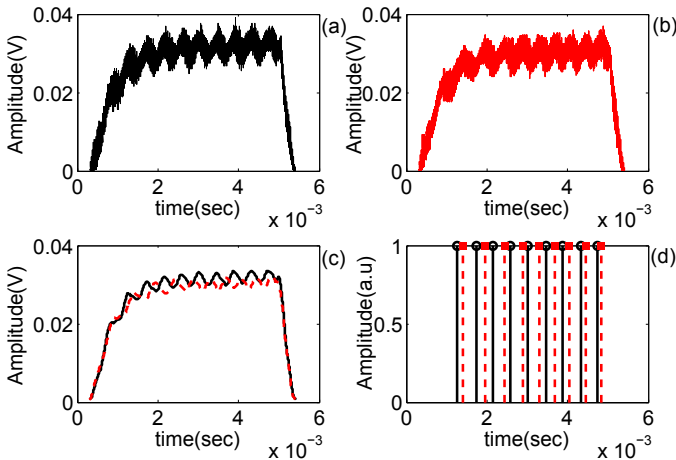
Fig. 4: Experimental results. (a) OFI signal, reference case, after differentiation for separating the fringes from the ramp in the acquired signal; (b) OFI signal, vibration case, also after differentiation (c) Denoised and differentiated OFI fringes for reference (solid line) and vibration (broken line) cases; (d) Shift in time occurrence of fringes in the vibration cases with respect to reference case that forms the basis of displacement calculation.
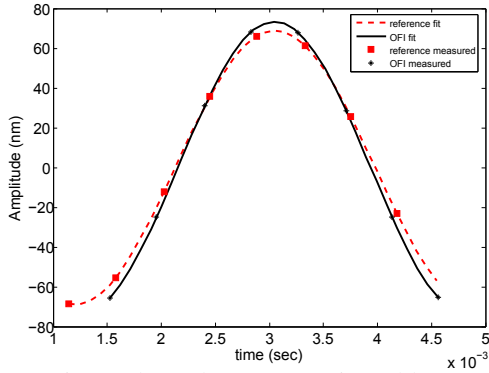

Fig. 5: Experimental results (Expt. 1 in Table II). Proposed OFI based target displacement compared against piezoelectric stage embedded capacitive sensor.

Since $p > \alpha_s$, we conclude that the data samples in OFI and Ref (Table II) have same mean at 95% confidence level. For illustration purposes, the first case, which had an error (pp) of 1.5 nm is shown in Fig. 5. In order to further prove the feasibility of the proposed methodology, it was applied to detect arbitrary waveform shapes. Results of experiments to measure Gaussian pulse shapes of width 4 ms and amplitude 63.8 nm are presented in Fig. 6, showing an average error (pp) of 4.05 nm measured under comparable conditions to that of Fig. 5. The relatively high error in Gaussian waveform is due to the limited number of sample points to follow rapid changes in the slope of the displacement giving rise to rapid phase changes (as compared to former).

IV. CONCLUSION

We have proposed and experimentally demonstrated a methodology to make efficient use of direct laser injection current modulation to induce CWFM and nonlinear dynamics effects in a LD subjected to optical feedback to measure nanometric amplitude displacements. The key contribution of this work is the use of single laser diode to detect sub

TABLE II: Experimental results.

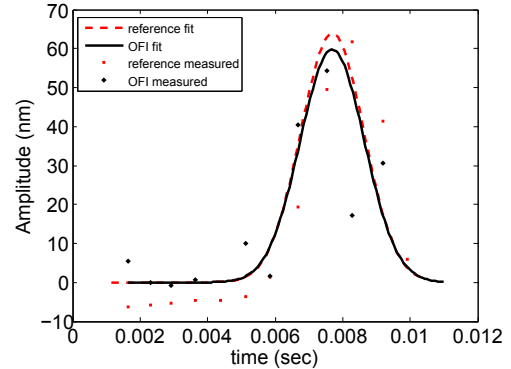| Expt.	Ref (nm)	OFI (nm)	Error (nm)
1	137.5	139.0	1.5
2	155.55	155.18	0.37
3	126.08	124.58	1.5
4	132.95	132.41	0.54
5	159.1	156.3	2.8

Fig. 6: Experimental results. Gaussian pulse detected compared against piezoelectric stage embedded capacitive sensor.

wavelength target vibrations with nanometric accuracies, using the modulation of the injection current and expanding the bandwidth of former DSMI sensors [7] to at least the MHz frequency range in detection. The mean peak to peak error of the proposed sensor out of nine different measurement of a single oscillation is 2.4 nm; a Gaussian pulse of width 4 ms and amplitude 63.8 nm is also detected with mean error (pp) of 4.08 nm. The maximum target vibration detectable is limited to $\lambda/2$, and the bandwidth of the sensor is proportional to the number of fringes and frequency of the laser current modulation.

REFERENCES

[1] R. Lang and K. Kobayashi, "External optical feedback effects on semiconductor injection laser properties," *IEEE J. Quantum Electron.*, vol. 16, pp. 347–355, March 1980.

[2] N. Jiang, W. Pan, B. Luo, L. Yan, S. Xiang, L. Yang, D. Zheng, and N. Li, "Influence of injection current on the synchronization and communication performance of closed-loop chaotic semiconductor lasers," *Opt. Lett.*, vol. 36, pp. 3197–3199, Aug 2011.

[3] S. Donati, G. Giuliani, and S. Merlo, "Laser diode feedback interferometer for measurement of displacements without ambiguity," *IEEE J. Quantum Electron.*, vol. 31, pp. 113–119, 1995.

[4] N. Servagent, F. Gouaux, and T. Bosch, "Measurement of displacement using self mixing interference in a laser diode," *J.opt*, vol. 29, pp. 168–173, Aug 1998.

[5] C. Bes, G. Plantier, and T. Bosch, "Displacement measurements using a self-mixing laser diode under moderate feedback," *IEEE Trans. Instrum. Meas.*, vol. 55, pp. 1101–1105, Aug 2006.

[6] D. M. Guo, M. Wang, and S. Q. Tan, "Self-mixing interferometer based on sinusoidal phase modulating technique," *Opt.Express*, vol. 13, pp. 1537–1543, Aug 2005.

[7] F. Azcona, R. Atashkhooei, S. Royo, J. Astudillo and A. Jha, "A nanometric displacement measurement system using differential optical feedback interferometry," *IEEE Photon. Technol. Lett.*, vol. 25, pp. 2074–2077, 2013.

[8] E. Gagnon and J.F. Rivest, "Laser range imaging using the self-mixing effect in a laser diode," *IEEE Trans. Instrum. Meas.*, vol. 48, pp. 693–699, June 1999.

[9] S. Kobayashi,Y. Yamamoto, M. Ito, T. Kimura,"Direct frequency modulation in AlGaAs semiconductor lasers, *IEEE J. Quantum Electron.*, vol.18, pp. 582-595, Apr 1982.

[10] http://www.physikinstrumente.com/product-detail-page/p-753-200900.html.

[11] D. Zhigang, Z. Jingxuan, and J. Chunrong, "An improved wavelet threshold denoising algorithm," Proc. *International Conference on Intelligent System Design and Engineering Applications*, pp. 297–299, China 2013.